Electrical Properties and Defect Chemistry of TiO_2 Single Crystal. II. Thermoelectric Power†

M. K. Nowotny, T. Bak, and J. Nowotny*

The University of New South Wales, Centre for Materials Research in Energy Conversion, School of Materials Science and Engineering, Sydney, NSW 2052, Australia

Received: January 29, 2006; In Final Form: May 11, 2006

The present work reports the thermoelectric power of high-purity single-crystal TiO_2 in the temperature range 1073−1323 K and in gas phases of controlled oxygen activities, $p(O_2)$, in the range 10^{-13} to 7.5×10^4 Pa. The thermoelectric power versus log $p(O_2)$ dependence for strongly reduced TiO_2 at $p(O_2) < 10^{-5}$ Pa may be approximated by a slope of 1/6, which is consistent with the defect disorder governed by electronic charge compensation of oxygen vacancies. The thermoelectric power data confirm that oxygen vacancies are the predominant ionic defects. These data indicate that TiO_2 at high $p(O_2)$ exhibits p-type properties. It is shown that the $p(O_2)$ related to the n−p transition increases with increase of temperature.

1. Introduction

The first paper of this series reports the electrical conductivity of TiO_2 single crystal at elevated temperatures in gas phases of controlled oxygen activities.[1] These data were considered in terms of defect disorder of TiO_2 within narrow regimes of oxygen activity.

Defect disorder of nonstoichiometric oxides has been studied mainly using the measurements of electrical conductivity.[2,3] However, electrical conductivity has a complex physical meaning because it includes both concentration and mobility terms.

Therefore, the synonymous interpretation of electrical conductivity data for oxide materials is difficult. Further, derived defect disorder models based on studies of a single property, such as electrical conductivity, should be verified using appropriate tests based on another property determined independently.

Thermoelectric power represents such an independent test method, as its use, in combination with electrical conductivity, allows differentiation between the concentration and mobility terms of the charge carriers.[4−6] It has been demonstrated that *simultaneous* measurements of both electrical conductivity and thermoelectric power at elevated temperatures (when studied oxide is in equilibrium with the gas phase) is useful in the quantitative assessment of the charge transport and thus for determination of the defect disorder, particularly in the n−p transition regime.[5,6]

At present, the reported thermoelectric power data for TiO_2 are both limited and contradictory.[4,7−9] The conflicting reports are mainly related to the following reasons: (1) Precision of the determination of the thermoelectric power data is not satisfactory. (2) Studied specimens are not well-defined in terms of the impurity level. (3) Experimental conditions are not well-defined in terms of the gas−solid equilibrium.

Therefore, the purpose of the present work is the determination of thermoelectric power for TiO_2 that is free of the above shortcomings. Specifically, the present work aims at achieving the following objectives: (1) The thermoelectric power will be determined with unprecedented precision using the dedicated facility. (2) The studied specimens will be high-purity TiO_2 single crystal. (3) The experimental data will be determined in equilibrium and evidence of the equilibrium will be achieved through the determination of the equilibration kinetics.[10] (4) Data reproducibity will be assessed within several independent experiments.

Data by the authors, aiming to assess the defect disorder, for the electrical conductivity of high-purity single-crystal TiO_2 are reported elsewhere.[1] The objective of the present work is to determine the thermoelectric power for the same TiO_2 specimen in identical experimental conditions and to assess the two sets of data in terms of the defect disorder and the related semiconducting properties.

2. Definition of Terms

2.1. Definition of Thermoelectric Power. The principle of determination of thermoelectric power is illustrated in Figure 1. The imposition of a temperature difference, ΔT, across a specimen with the use of, for example, microheaters attached to the specimen, results in the generation of an electrical potential difference, ΔV, which is termed the *thermoelectric voltage* (or *thermovoltage* or *Seebeck voltage*). Knowledge of both ΔV and ΔT are required to determine the *thermoelectric power*, (or *thermopower* or *Seebeck coefficient)*, S:[5]

$$S = \frac{\Delta V}{\Delta T}\,[V \cdot K^{-1}] \tag{1}$$

The sign of S is determined by the conductivity type and adopts negative and positive values for n- and p-type conductors, respectively. Equation 1 is valid when: the thermoelectric power is independent of the applied temperature

† This project was performed as part of a UNSW R&D program on solar−hydrogen.

* Corresponding author. E-mail: J.Nowotny@unsw.edu.au. Telephone: 612-9385.6465. Fax: 612-9385.6467.

10.1021/jp060622s CCC: $33.50
Published on Web 08/01/2006

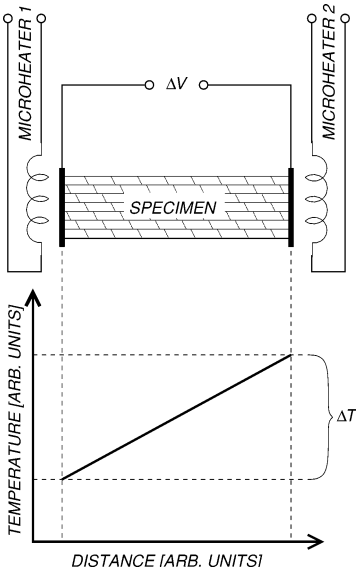

Figure 1. Principle of determination of thermoelectric voltage, ΔV, along a temperature gradient, ΔT.

gradient, and the studied solid is of uniform composition and microstructure, consequently giving a constant temperature gradient.

When the thermoelectric power depends on the temperature gradient, its correct determination requires the following condition:[3]

$$S = \lim_{\Delta T \to 0} \frac{\Delta V}{\Delta T} = \frac{dV}{dT} \tag{2}$$

Therefore, it is advantageous for S to be measured at small ΔT. It should be noted that the smallest ΔT that can be used is determined by the sensitivity limit of the equipment used to determine the Seebeck voltage. In practice, the minimal ΔT values that can be used are in the range 2−5 K.

The absolute value of the S depends on the nature of the solid, its chemical composition, microstructure (single crystal versus polycrystal), and temperature. For semiconducting solids, S can reach levels of several hundred $\mu V/K$ while metallic solids have much lower levels.

For n- and p-type regimes, the following equations describe relations between S and the concentrations of electronic charge carriers:[5]

$$S_n = -\frac{k}{e}\left(\ln\frac{N_n}{n} + A_n\right) \tag{3}$$

$$S_p = \frac{k}{e}\left(\ln\frac{N_p}{p} + A_p\right) \tag{4}$$

where the subscripts n and p refer to electrons and electron holes, respectively, k is Boltzmann's constant, e is the elementary charge, N is the density of states, n and p are the concentrations of electrons and electron holes, respectively, and A is a parameter describing the scattering mechanism of the charge carriers.

It can be seen from the eqs 3 and 4 that S is independent of the mobility terms (μ_n or μ_p). Therefore, the combination of data for both thermoelectric power and electrical conductivity, which includes the mobility terms, allows separation and assessment of the concentration and mobility terms individually when both properties are determined under identical conditions.[5]

Because the experimental determination of the mobility is very difficult, especially at elevated temperatures, then the formalism proposed by Jonker,[11] which yields the mobility terms and the band gap, represents an advantageous approach to define the relevant semiconducting quantities.

2.2. Effect of Oxygen Activity on Thermoelectric Power of Oxide Semiconductors. Electrical properties, such as electrical conductivity and thermoelectric power, in nonstoichiometric oxides, are a reflection of the concentrations of electronic charge carriers.[2−5] Further, their concentrations are a reflection of the nonstoichiometry, the associated oxygen activity, and the related defect disorder.[2] Therefore, measurements of the electrical properties may be used to verify the defect disorder models of metal oxides. The effect of the oxygen activity, $p(O_2)$, on the electrical conductivity, σ, and thermoelectric power, S, are described by the following respective relationships:

$$\frac{1}{m_\sigma} = \frac{\partial \log \sigma}{\partial \log p(O_2)} \tag{5}$$

$$\frac{1}{m_S} = \frac{k}{e}\frac{\partial S}{\partial \log p(O_2)} \tag{6}$$

where m_σ and m_S are parameters that reflect the nature of the defect disorder when determined using measurements of the electrical conductivity (m_σ) or thermoelectric power (m_S). The sign of m_S in both n- and p-type regime is positive.

The thermoelectric power assumes a critical value of zero at a $p(O_2)$ corresponding to the n−p transition. The parameter m_S is determined from the slope of the linear part of an S versus log $p(O_2)$ plot. Comparative analysis of the effect of the $p(O_2)$ on σ and S is possible when both properties are established by the same type of predominant charge carrier (electrons or electron holes) and in identical conditions of the gas−solid equilibrium. Then the values of the slopes of these two sets of data may be considered in terms of the defect disorder.[4−6]

In the present study, the following $p(O_2)$ regimes are considered:[1] (i) Strongly Reduced Regime. This regime is consistent with defect disorder based on doubly ionized oxygen vacancies, which are compensated by electrons, as the predominant defect. The S versus log $p(O_2)$ dependence in this $p(O_2)$ regime is approximated by a slope of 1/6 when the predominant charge carriers are electrons. This regime is governed by electronic charge compensation that requires that:[1]

$$n = 2[V_O^{\bullet\bullet}] \tag{7}$$

(ii) Reduced Regime. The predominant ionic defects in this regime also are doubly ionized oxygen vacancies, although, in this case, they are compensated by titanium vacancies:[1]

$$[V_O^{\bullet\bullet}] = 2\,[V_{Ti}^{''''}] \tag{8}$$

The predominant electronic charge carriers in this regime are electrons. The S versus log $p(O_2)$ dependence in this $p(O_2)$ regime is approximated by a slope of 1/4. However, this precise slope for undoped TiO_2 is not observed owing to the effect of the minority charge carriers on thermoelectric power. (iii) Oxidized Regime. This regime is governed by the same charge compensation as that in the reduced regime, which are determined by eq 8, although the predominant electronic defects are electron holes. The $p(O_2)$ exponent in this regime is 1/4 when the predominant electronic charge carriers are electron holes[1].

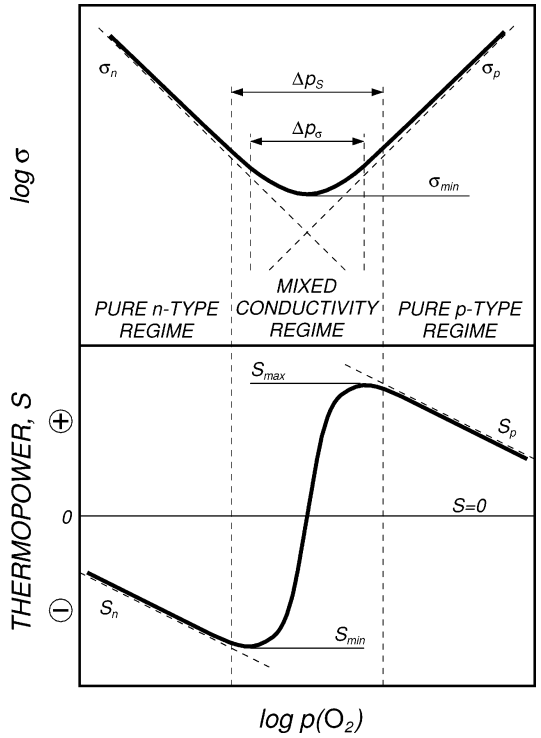

Figure 2. Schematic representation of the effect of $p(O_2)$ on the electrical conductivity, σ, and thermoelectric power, S, of oxide semiconductors within the n−p transition.

Again, this slope is not observed for undoped TiO_2 owing to the effect of the minority charge carriers on thermoelectric power.

Figure 2 illustrates schematically plots of σ and S versus log $p(O_2)$ for an amphoteric semiconductor (showing both n- and p-type behavior), such as TiO_2, in the vicinity of the n−p transition. There are generally three regimes that can be identified: (i) The n-Type Regime. As seen in Figure 2, the slopes of the linear dependencies log σ versus log $p(O_2)$ and the slope S versus log $p(O_2)$ are the same if the measurements are performed in identical conditions, assuming that the data are free of the minority charge carrier. (ii) The n−p Mixed Conductivity Regime. As seen, the effect of $p(O_2)$ on the σ and S in this regime is entirely different. Here, the log σ versus log $p(O_2)$ and the S versus log $p(O_2)$ dependencies exhibit more complex characteristics. It is important to note that the $p(O_2)$ ranges for the transition, determined from the S (Δp_S) or σ (Δp_σ), are not identical. In this regime, where the $p(O_2)$ slopes exhibit a complex change within $p(O_2)$, the wider of these two $p(O_2)$ ranges is subject to greater contribution from the minority charge carrier. Therefore, the $p(O_2)$ slope in this regime is not suitable for assessment of defect disorder. (iii) The p-Type Regime. The slopes of log σ versus log $p(O_2)$ and S versus log $p(O_2)$ should be the same if the data are obtained under identical conditions and if both σ and S are not affected significantly by the minority charge carriers. Experimental data in this regime have been considered for $BaTiO_3$.[5] So far, the data reported in this regime for TiO_2 are scarce and conflicting.

As seen in Figure 2, the S versus log $p(O_2)$ dependence involves several characteristic points, including maximum (S_{max}), minimum (S_{min}), and inflection point (where $S = 0$). The latter point demarcates the n- and the p-type regimes.

In cases when the mobilities of both electronic charge carriers are the same, then the $p(O_2)$ corresponding to $S = 0$ is identical to that corresponding to the minimum of electrical conductivity (σ_{min}):

$$p(O_2)_{S=0} = p(O_2)_{\sigma(min)}; \qquad \text{when } \mu_n = \mu_p \qquad (9)$$

When eq 9 applies, there is symmetry between the two sets of data. Such symmetry is not always the case.

The purpose of the present work is to determine the effects of $p(O_2)$ on the S of high-purity single-crystal TiO_2 and to assess the data for both the σ and S in terms of the defect disorder and the associated semiconducting properties.

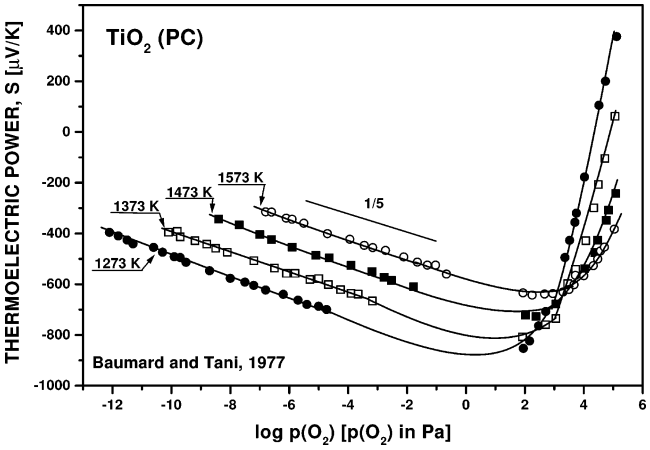

Figure 3. Thermoelectric power as a function of oxygen activity for TiO_2 single crystal according to Baumard and Tani.[4]

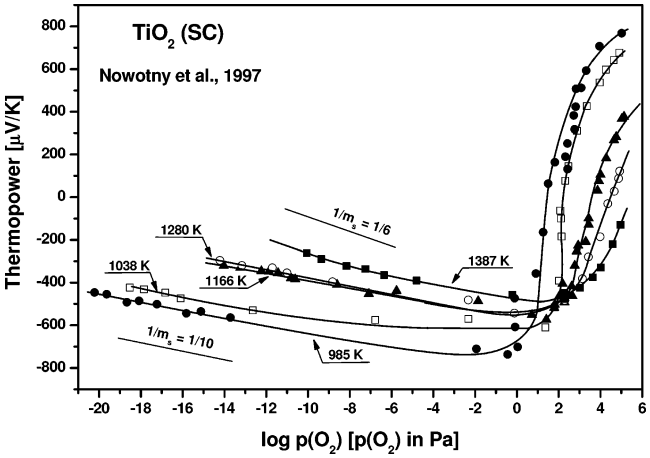

Figure 4. Thermoelectric power as a function of oxygen activity for TiO_2 single crystal according to Nowotny et al.[7]

3. Brief Literature Overview

Reports of the use of thermoelectric power to study the defect disorder of undoped TiO_2 are limited.[4,7−9] Further, there are considerable discrepancies between the data, particularly for the $p(O_2)$ exponent and the n−p transition point.

The use of thermoelectric power to study the defect disorder of reduced TiO_2 was reported by Baumard and Tani[4] and Nowotny et al.[7] These data are shown in Figures 3 and 4, respectively. Other data were reported either at unknown $p(O_2)$[8] or in the high $p(O_2)$ in which the thermoelectric power data are influenced strongly by the minority charge carriers.[9]

The thermoelectric power data at high temperatures was reported first by Baumard and Tani[4] for polycrystalline TiO_2 (TiO_2-PC). Their $p(O_2)$ exponent data, which covered the temperature range 1273−1573 K and $p(O_2)$ range 10^{-12} to 10^5 Pa, for TiO_2 reduced below 10^{-2} Pa, was 1/5. Their experimental

data indicate that undoped TiO_2 exhibits n-type properties ($S < 0$) over nearly the entire range of $p(O_2)$ studied, except at the highest $p(O_2)$ (log $p(O_2) > 4.5$). The 1/5 exponent, which is well consistent with their data of the electrical conductivity, they consider in terms of tetravalent Ti interstitials as the predominant defects in this regime, which are formed according to the following equilibrium:

$$Ti_{Ti}^{x} + 2O_{O}^{x} \rightleftarrows Ti_{i}^{\bullet\bullet\bullet\bullet} + 4e' + O_2 \tag{10}$$

Then the charge neutrality requires that:

$$4[Ti_{i}^{\bullet\bullet\bullet\bullet}] = n \tag{11}$$

Therefore:

$$n = (4K_{Ti(+4)})^{1/5}\, p(O_2)^{-1/5} \tag{12}$$

where:

$$K_{Ti(+4)} = [Ti_{i}^{\bullet\bullet\bullet\bullet}]\, n^4\, p(O_2) \tag{13}$$

While the $p(O_2)$ exponent reported by Baumard and Tani[4] is theoretically consistent with the above defect disorder model, this model is inconsistent with the defect disorder diagram reported by Kofstad.[2] The latter author indicates that the predominant defects in strongly reduced and extremely reduced TiO_2 are oxygen vacancies and trivalent Ti interstitials, respectively. The respective $p(O_2)$ exponent of σ is $-1/6$ and $-1/4$. There is a need to clarify the discrepancy between these conflicting reports.

The thermoelectric power data reported by Nowotny et al.[7] for undoped single-crystal TiO_2 (TiO_2-SC) were obtained for temperatures of 985−1387 K and $p(O_2)$ of 10^{-20} to 10^5 Pa. These data indicate that the specimen exhibits the n−p transition point, which varies between log $p(O_2) = 1.5$ at 985 K and log $p(O_2) = \sim 5$ at 1280 K. Further, the determined $p(O_2)$ exponent in this work varies between 1/6 and 1/10 at 1385 and 985 K, respectively. However, as seen in Figure 4, these data exhibit a substantial scatter. Therefore, these data also require a verification.

Kuratomi et al.[8] reported data for the thermoelectric power versus electrical conductivity for undoped TiO_2-PC in the temperature range 1023−1223 K. While these data were determined simultaneously in identical $p(O_2)$, the actual $p(O_2)$ values were not measured. Therefore, these data do not allow assessment of the $p(O_2)$ exponent of the thermoelectric power. However, application of the Jonker analysis[11] to these data indicated a clear n−p transition at all temperatures. The n−p transition was confirmed by Bak et al.,[9] who also studied TiO_2-PC; however, their data were reported in the high $p(O_2)$ regime, $p(O_2) > 10$ Pa. Therefore, these data, which are influenced by both electronic charge carriers, are not appropriate for the assessment of defect disorder.

The analysis of the reported thermoelectric power data indicates that the determination of well-defined data of S requires the following issues to be addressed: (1) Polarization effects should be assessed using imposition of temperature gradients of two different polarities. (2) High accuracy may be achieved through (a), the determination of S as an average from measurements at several temperature gradients (40−50) and the related thermovoltages, and (b), the use of dedicated equipment, which allows precise determination of both ΔV and ΔT used for the determination of S. (3) Data must be measured in thermal equilibrium. This requires knowledge of gas−solid equilibration kinetics and the related chemical diffusion coefficient.[10]

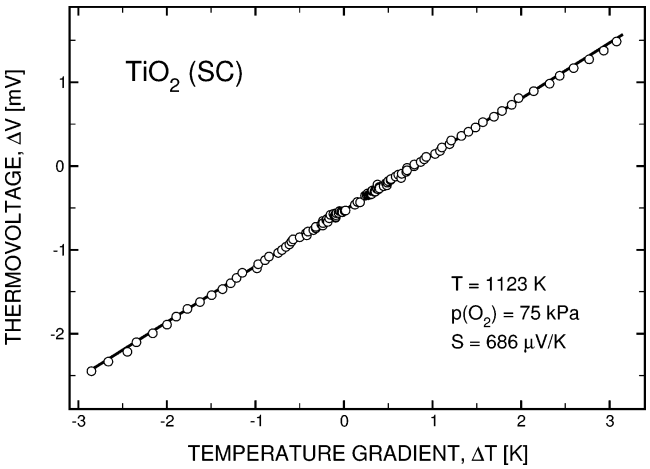

Figure 5. Experimental plot of thermovoltage, ΔV, along the temperature gradient, ΔT for TiO_2 single crystal at 1123 K, and $p(O_2) = 75$ kPa.

The purpose of the present work is the determination of such data for high purity TiO_2 single crystal and their analysis along the electrical conductivity data.

4. Experimental Procedure

The undoped TiO_2 single crystal (TiO_2-SC) used in the present work has been described before.[1] Both the thermoelectric power and electrical conductivity were determined simultaneously using a high-temperature Seebeck probe.[5] Its recent modification allows the determination of thermopower with higher precision due to the following arrangements: (i) Application of a data processing program that allows the measurements of thermoelectric power along the temperature difference using two different polarities, ΔT and $-\Delta T$, for 40−50 different temperature gradients in the range 0−5 K. (ii) Application of a data acquisition program that allows simultaneous and continuous monitoring of several experimental conditions of importance for the determination of thermoelectric power, including temperature, oxygen activity, and electrical conductivity. These data are essential for appropriate assessment of the thermoelectric power data. (iii) Application of a new system of microheaters that allow imposition of controlled temperature microgradients.

The thermoelectric power was determined from the slopes of independent measurements of the thermoelectric voltage. The temperature gradient was imposed by two microheaters, which were attached to both sides of the specimen. To achieve good data reproducibility, the thermoelectric power was determined after the studied specimen reached thermal equilibrium. Figure 5 shows the typical slope of thermovoltage vs temperature gradient. In consideration of the uncertainty associated with the determination of ΔT (± 0.1 K) and that of the thermoelectric voltage ($\pm 1\%$), the temperature variation of the individual determinations was within $\pm 1\%$. Other details of this procedure are reported elsewhere.[1]

The thermoelectric power, S, of an oxide specimen is determined by adding the absolute thermoelectric power of the Pt electrode, S_{Pt}, to the experimentally determined value of the thermoelectric power, S_{exp}:

$$S = S_{exp} + S_{Pt} \tag{14}$$

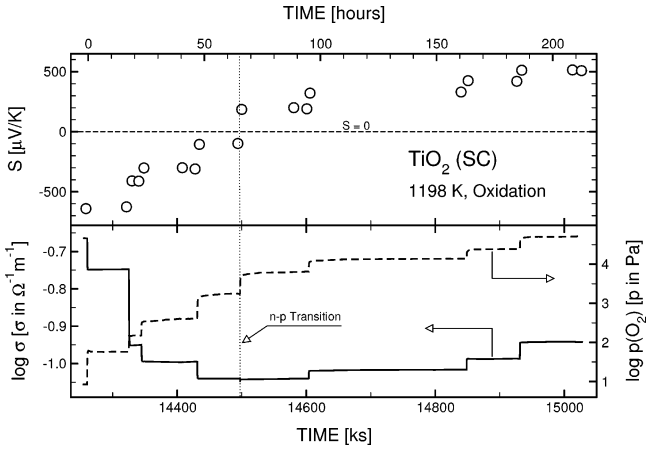

Figure 6. Experimental monitoring sheet showing the change of thermoelectric power (this work) and electrical conductivity[1] for TiO_2 single crystal during an oxidation experiment at 1198 K.

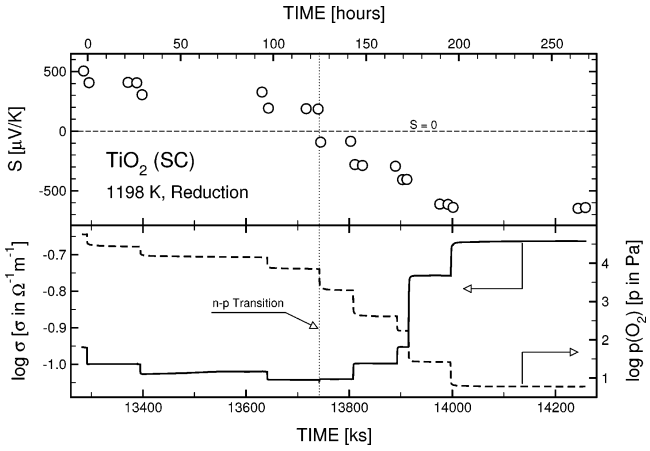

Figure 7. Experimental monitoring sheet showing the change of thermoelectric power (this work) and electrical conductivity[1] for TiO_2 single crystal during a reduction experiment at 1198 K.

The absolute value of the thermoelectric power of the Pt electrode in the range 100−2000 K was determined by Cusack and Kendall:[13]

$$S_{Pt} = -2.63 - 0.0145\,T \qquad [\mu V/K] \qquad (15)$$

Identical experimental conditions were used for the determination of the electrical conductivity.[1] In both cases, the temperature range was 1073−1323 K and the oxygen activity in the gas phase was imposed by argon/hydrogen and argon/oxygen mixtures, which yielded $p(O_2)$ levels in the ranges $\sim 10^{-12}$ to 10^{-5} Pa and $\sim 10^{1}$ to 10^{5} Pa, respectively.

5. Results and Discussion

5.1. Changes in Electrical Conductivity and Thermoelectric Power during Oxidation and Reduction. Figures 6 and 7 illustrate representative monitoring sheets that show the changes in both electrical conductivity and thermoelectric power as a function of time during oxidation and reduction experiments, respectively. Both oxidation and reduction were performed using small changes in $p(O_2)$.

The measurement within the small changes in $p(O_2)$ was essential because there are substantial changes in the properties of TiO_2 as a function of $p(O_2)$, including defect disorder and the defect-related properties, such as thermoelectric properties. The lower part of Figure 6 shows that, despite a stepwise increase in the $p(O_2)$, the corresponding stepwise changes in the electrical conductivity show an inflection in behavior. The minimum, which correspond to the n−p transition point, allows determination of the $p(O_2)$ of the transition. The upper part of Figure 6 shows the effect of the $p(O_2)$ on the thermoelectric power. It can be seen that increasing the $p(O_2)$ leads to a continuous increase in the thermoelectric power, which passes through zero at the n−p transition point. The correspondence between the minimum in the electrical conductivity and reversal of the sign of the thermoelectric power indicates that the mobilities of the electronic charge carriers at this temperature are the same. Comparison of the data in Figure 6, which are for oxidation, with those shown in Figure 7, which are for reduction, demonstrates consistency between the two experimental conditions. This observation indicates that the data correspond to conditions of operational equilibrium that are related to the kinetic regime I,[14] which is determined by the transport of oxygen vacancies. Therefore, the present work will ignore the electrical phenomena in the kinetic regime II, which are related to the formation and transport of titanium vacancies,[14] because in the experimental conditions applied in this work, the related processes are quenched.

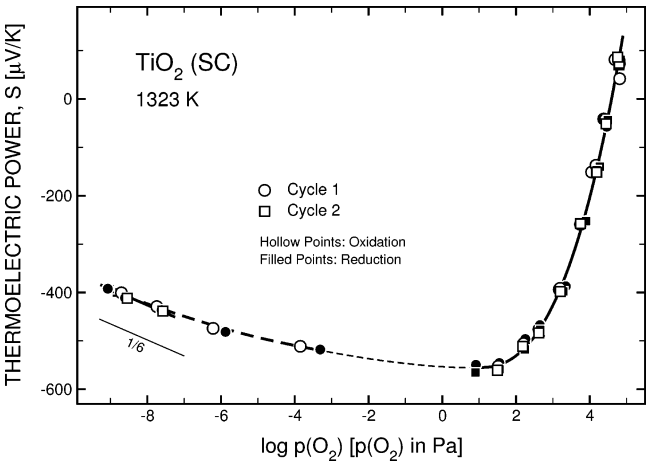

Figure 8. Effect of oxygen activity on thermoelectric power for TiO_2 single crystal during both reduction and oxidation at 1323 K showing the reproducibility of data within two independent experiments.

5.2. Effect of Oxygen Activity on Thermoelectric Power. Figure 8 shows the reproducibity of effect of the $p(O_2)$ on the thermoelectric power during oxidation and reduction within the entire $p(O_2)$ regime at 1323 K during two independent experimental cycles, both including oxidation and reduction experiments. It is clear that the data are quite reproducible, thereby confirming the presence of the conditions of both thermal and chemical equilibrium. Consequently, the data in Figure 8 indicate that the applied experimental procedure allows the determination of well-defined thermoelectric power. The experimental data for the thermoelectric power for the entire temperature range in the low $p(O_2)$ range are shown in Figure 9. This figure also includes the thermoelectric power data for high-purity polycrystalline TiO_2 (TiO_2-PC) determined at 1273 K using the same equipment and following the same experimental procedure.[15]

The data in Figures 8 and 9 exhibit a continuous change of the S vs log $p(O_2)$ slope from 1/6 at extremely reduced conditions to smaller $1/m_S$ values. These effects of $p(O_2)$ on S may be considered in terms of the following alternative explanations: (1) The data at the extremely reduced conditions are consistent with the model predicted for the strongly reduced regime. The gradually decreasing slope indicates increasing

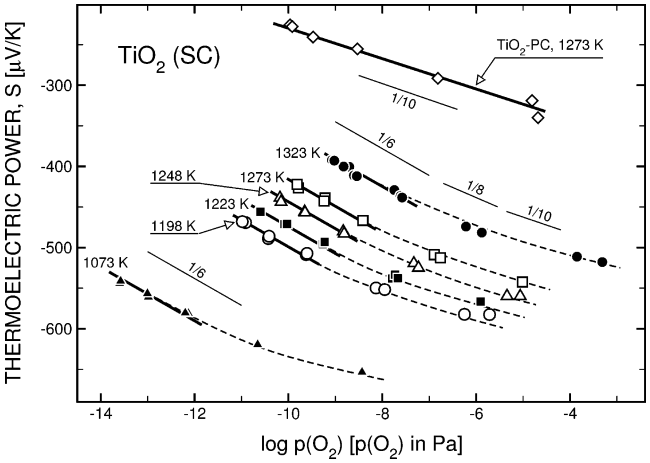

Figure 9. Effect of oxygen activity on thermoelectric power for TiO_2 single crystal during both reduction and oxidation in the entire temperature range showing the experimental data in the low oxygen activity regime.

influence of the minority charge carriers. Therefore, only the linear part corresponding to $1/m_S = 1/6$ at the most reduced conditions is appropriate for the interpretation in terms of a defect model related to pure n-type conduction. (2) An alternative approach is to approximate the observed curvature of S vs log $p(O_2)$ within a wider $p(O_2)$ regime in terms of a linear dependence, of which the slope is close to 1/8. However, in terms of the achieved high accuracy of the determined S in the present work, there is a need to distinguish the slope 1/6 in extremely reduced conditions and the smaller slope at larger $p(O_2)$. The latter one cannot be easily explained in terms of any TiO_2 defect model. The alternative explanation of the odd slope value of 1/8 is the contribution of minority charge carriers.

As seen in Figure 9, the slope of the thermoelectric power versus log $p(O_2)$ dependence for polycrystalline TiO_2 (TiO_2-PC) is less than 1/6. The slope $1/m_S$ at 1273 K is ~1/10 in the entire low $p(O_2)$ regime (similar slope was determined in the entire temperature range). Because in both cases of TiO_2-PC and TiO_2-SC the specimens were of high purity, the only difference between the two is the presence of grain boundaries for TiO_2-PC.

Why is S of TiO_2-PC specifically sensitive to grain boundaries? The effect of grain boundaries may be considered in terms of the model reported by Parravano and Domenically,[16] which is schematically represented in Figure 10. As seen in the upper part of Figure 10, the temperature distribution in a polycrystalline specimen is not uniform. Then thermoelectric power may be considered in terms of the following two components:

$$S = S_{\text{bulk}} + S_{\text{gb}} \tag{16}$$

where S_{bulk} and S_{gb} denote the thermoelectric power components related to the bulk of grains and grain boundaries. Specifically, the temperature gradient within the bulk of the grain is lower than that at grain boundaries owing to their lower thermal conductivity. In consequence, the thermoelectric power measurement for a polycrystalline specimen is predominantly sensitive to their grain boundaries. Because the local defect chemistry and the related properties of grain boundaries are entirely different than those of the bulk, the thermoelectric power for polycrystalline specimen and single crystal of the same compound may differ substantially. On the other hand, as seen in the lower part of Figure 10, the temperature distribution within single crystal is uniform. Then thermoelectric power is purely bulk property. Consequently, the slope 1/10 observed for TiO_2-PC is a reflection of the defect disorder of the grain boundary region.

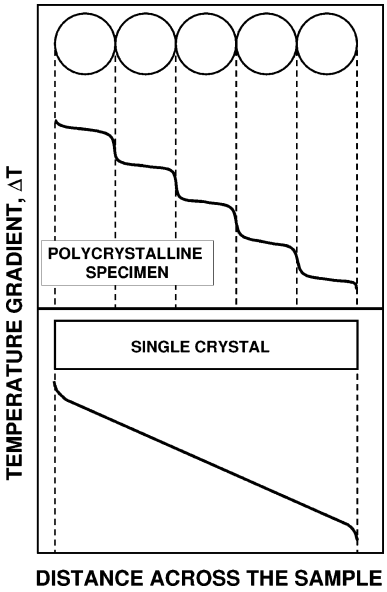

Figure 10. Schematic representation of the temperature profile across polycrystalline specimen according to Parravano and Domenically.[16]

What is the specific property of grain boundaries that may lead to such a strong change of the slope? There is no simple defect disorder model for TiO_2, which may be consistent with the slope $1/m_S = 1/10$. One may expect, however, that the surface layer of metal oxides, including TiO_2, differs from the bulk phase not only in terms of defect disorder but also in terms of the structure due to the following reasons: (1) segregation of defects, such as oxygen vacancies, leads to the formation of concentration gradients within the surface layer,[17] and (2) the segregation-induced enrichment results in substantial interactions between the defects, leading to the formation of larger defect aggregates[18] and, ultimately, to the formation of low-dimensional interface structures.[19]

Explanation of the effect observed for TiO_2-PC requires "in situ" examination of the local surface properties of TiO_2.

At higher $p(O_2)$ levels, the data in Figure 9 deviate from 1/6 linearity. This deviation, which increases with increase of $p(O_2)$ (ultimately leading to the slope equal to zero) indicates that the S data are affected by the minority charge carriers (electron holes). Their influence ultimately leads to the n−p transition, which was revealed to be in the high $p(O_2)$ range, as shown in Figure 11.

The effects of $p(O_2)$ on the thermoelectric power for the entire ranges of temperature and $p(O_2)$ are shown in Figure 11. These data, which also include data for TiO_2-PC at 1273 K,[15] indicate the following: (i) At the midrange $p(O_2)$, the slope of the thermoelectric power versus log $p(O_2)$ dependence changes continuously at all temperatures. The thermoelectric power data in this regime are influenced by both electrons and holes and, therefore, are not appropriate for the consideration in terms of defect disorder. (ii) Increase of $p(O_2)$ leads to a minimum of thermoelectric power and subsequent dramatic increase by ~1000 μV/K. At the highest $p(O_2)$ at each temperature, the thermoelectric power is positive, indicating the formation of p-type TiO_2 at the highest $p(O_2)$. (iii) The formation of p-type TiO_2 requires the presence of acceptors. Because the only feasible intrinsic acceptor-type defects in high-purity TiO_2 used in the present study are titanium vacancies, these defects are the only explanation of the p-type TiO_2. That is, this effect cannot be explained by the so-called *extrinsic model*, which

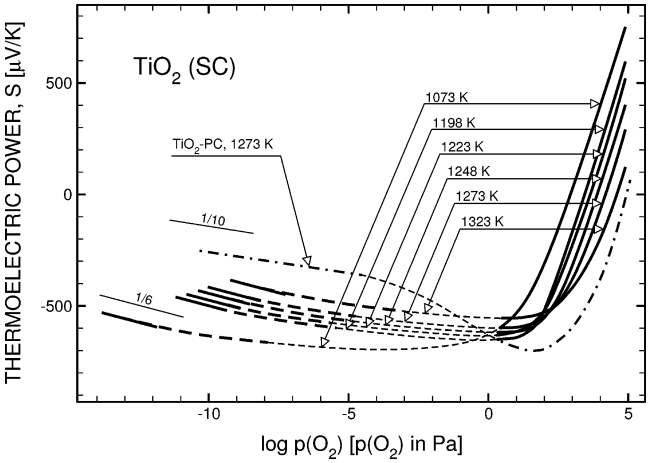

Figure 11. The effect of oxygen activity on thermoelectric power for TiO_2 single crystal during both reduction and oxidation in the temperature range 1073−1323 K; thick solid lines represent the best approximation of experimental data, thin dashed lines represent the extrapolated dependence (data for polycrystalline TiO_2 are shown as a reference).

assumes the presence of acceptor-type impurities and/or dopants.[20,21] (iv) Decrease of $p(O_2)$ results in minimization of the effect of electron holes on the thermoelectric power for TiO_2-SC, which becomes a purely n-type semiconductor at the extremely reduced conditions where the S versus log $p(O_2)$ dependence exhibits a slope of 1/6. This slope is consistent with the strongly reduced regime model.[1]

To assess the thermoelectric power data in terms of the n−p transition, the experimental data now are compared to electrical conductivity data reported elsewhere.[1]

It will be shown subsequently that the slope of 1/6 in the S versus log $p(O_2)$ data for extremely reduced TiO_2 is in agreement with the same slope in the log σ vs log $p(O_2)$ data, although in the latter case, the slope covers a wider $p(O_2)$ range. These two confirmatory sets of data indicate that the predominant ionic defects in reduced TiO_2 in this $p(O_2)$ regime are oxygen vacancies that are compensated by electrons.[1] Further, these data indicate that Ti interstitials, which are considered to form in extremely reduced TiO_2,[2,12] remain the minority defects. According to the defect diagram in Figure 12, these defects are expected to be the predominant defects at 1273 K at $p(O_2) < 10^{-12}$ Pa.[12]

5.3. Thermoelectric Power Versus Electrical Conductivity. Figures 13 and 14 show the data for the electrical conductivity (upper parts) and thermoelectric power (lower parts) as a function of $p(O_2)$ at two different temperatures. The slopes from the electrical conductivity and thermopower data compared in Figures 13 and 14 indicate that the absolute value of the slopes of the electrical conductivity versus $p(O_2)$ is 1/6. This value is in agreement with the defect disorder, which is governed by the following charge neutrality:

$$n = 2[V_O^{\bullet\bullet}] \tag{17}$$

The data in Figures 13 and 14 indicate the following: (i) The n−p transition point corresponds to both a thermoelectric power of zero and a minimum in the electrical conductivity. As seen in Figure 14, the $p(O_2)$ corresponding to the n−p transition point according to thermoelectric power is slightly lower than that according to the electrical conductivity. This may suggest that the mobilities of electrons and holes are not identical.[14] (ii) The slope of the $p(O_2)$ dependence related to the defect disorder model in a strongly reduced regime, 1/6, is

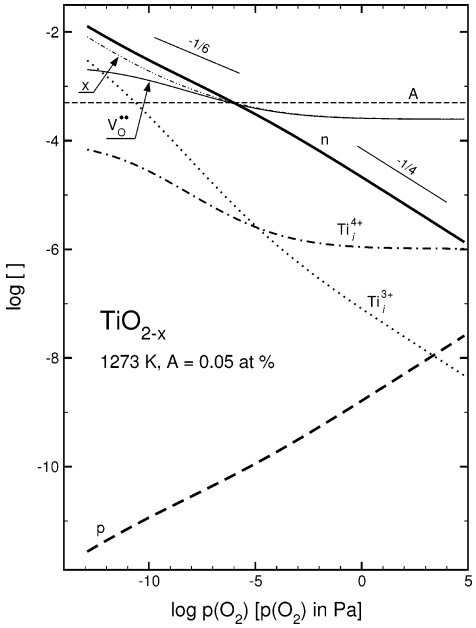

Figure 12. The diagram, derived based on equilibrium constants reported elsewhere,[1,12] showing the effect of oxygen activity on defect concentrations for TiO_2 at 1273 K and the concentration of acceptor A = 0.05 at. % (Ti vacancies); the square bracket on the y axis denotes molar concentration.

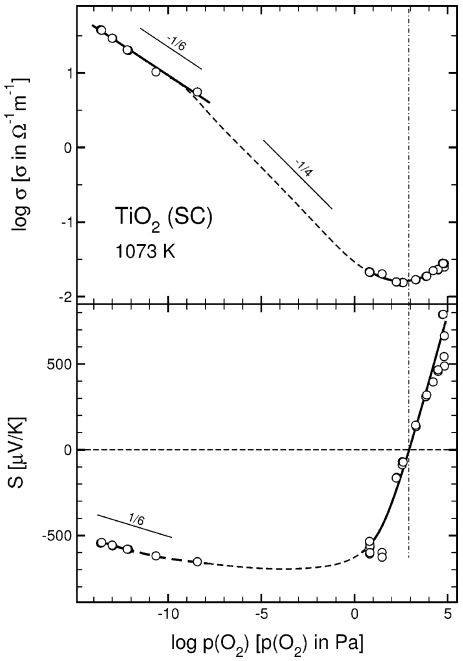

Figure 13. Electrical conductivity (upper part) and thermoelectric power (lower part) as a function of oxygen activity at 1073 K.

in agreement with the electrical conductivity data within relatively wide $p(O_2)$ regimes of 10^{-14} to 10^{-9} Pa and 10^{-9} to 10^{-4} Pa at 1073 and 1323 K, respectively. (iii) The slope of the $p(O_2)$ dependence related to the defect disorder model in a strongly reduced regime, 1/6, is in agreement with the thermoelectric power data within relatively narrow $p(O_2)$ regimes of 10^{-14} to 10^{-12} Pa and 10^{-9} to 10^{-7} Pa at 1073 and 1323 K, respectively. The slopes of the $p(O_2)$ dependence of the thermoelectric power at higher $p(O_2)$ cannot be represented simplistically as a function of the predominant charge carriers.

As seen in Figures 13 and 14, the slope of the thermopower vs $p(O_2)$ for the strongly reduced TiO_2, $1/m_S = 1/6$, which is

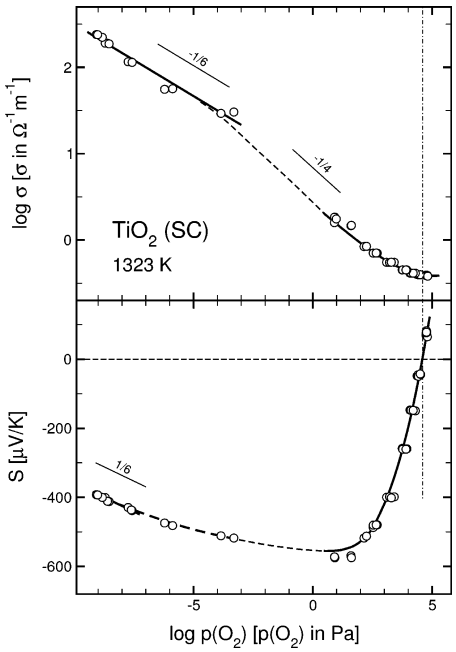

Figure 14. Electrical conductivity (upper part) and thermoelectric power (lower part) as a function of oxygen activity at 1323 K.

well consistent with the electrical conductivity data, differs from those reported before.[4,7−9] The differences between the data determined in the present work and the data reported before[4,6−9] can be considered in light of the following considerations: (i) Effects of Impurities. The effects of impurities are very important in the determination of electrical properties, including thermoelectric power, due to the changes of semiconducting properties caused by the incorporation of aliovalent ions forming donors and acceptors. (ii) Effects of Grain Boundaries. The segregation-induced concentration gradients across the grain boundaries of polycrystalline solids alters the local defect chemistry and the associated semiconducting properties. Consequently, as indicated in Figure 10, thermoelectric power is very sensitive to grain boundaries. (iii) Effects of Titanium Vacancies. It has been shown that titanium vacancies are formed during the processing (crystal growth) of undoped TiO_2.[14] It also has been shown that, due to kinetic reasons, these vacancies exhibit concentration gradients at both the grain boundaries and at the specimen surfaces. Because they affect the defect disorder, they also must affect the measured thermoelectric power.

It is surprising that the data of Burg[15] for a well-defined TiO_2-PC specimen show a $p(O_2)$ exponent of 1/10 instead of 1/6 determined in the present work for TiO_2-SC in the pure n-type regime. Because both TiO_2-PC and TiO_2-SC were of high purity, the difference between the two slopes (1/10 versus 1/6) reflects the effect of grain boundaries, as demonstrated by the sensitivity of thermoelectric power measurements to the effects of grain boundaries shown in Figure 10.

Baumard and Tani[4] reported the slope of 1/5 for their TiO_2-PC in the entire reduced regime. These authors attributed their slope (1/5) to the intrinsic effect of interstitial Ti^{4+}. This slope value has not been confirmed in the present study. The difference between the two sets of data may be considered in the following terms: (i) The concentration of impurities in the specimen studied in the present work and the PC specimen studied by Baumard and Tani[4] is 32 and 225 ppm, respectively. It seems, therefore, that the data of Baumard and Tani have overlaid effects from both ionic impurities and grain boundaries. The effect of the impurities depends on their impact on electronic structure. This may explain the value of 1/5 reported by Baumard and Tani.[4] (ii) There is no experimental evidence that the data of Baumard and Tani[4] were determined in equilibrium. If these data were determined in the kinetic regime, then the related effect may be responsible for the difference in the slope.

Nowotny et al.[7] reported the $p(O_2)$ slope, which varied between $1/m_S = 1/10$ at 985 K to 1/6 at 1387 K for TiO_2-SC. While the specimen was relatively pure (~50 ppm of impurities), the related data exhibited a large scatter, which most likely is due to the fact that the facility used in this study and the applied procedure did not allow the achievement of precision as high as that achieved in the present work. The scatter did not allow accurate assessment of the $p(O_2)$ dependence. It is interesting to note, however, that the slope $1/m_S$ at the highest temperature (1387 K) was close to 1/6.

6. Conclusions

The established effect of oxygen activity on thermoelectric power may be approximated by the slope of the S vs log $p(O_2)$ dependence, which is 1/6. This approximation, however, is limited to narrow $p(O_2)$ regimes, which are free of minority charge carrier influence. This slope corresponds to the strongly reduced regime.

The thermoelectric power data reported in the present work is well consistent with the electrical conductivity data determined simultaneously.[1] In the case of thermoelectric power data, the consistency is limited to the most reduced conditions. Nevertheless, the consistency indicates that the predominant defects in strongly reduced TiO_2 are oxygen vacancies that are compensated by electrons.

The comparison between the thermoelectric power data for TiO_2 single-crystal studied in the present work and the data for polycrystalline TiO_2 reported elsewhere[15] indicates that, in the latter case, the slope of the S vs log $p(O_2)$ dependence may be approximated by the value of 1/10 rather than 1/6. This effect is related to the presence of grain boundaries and their impact on the thermoelectric power of polycrystalline specimens. These data indicate that the physical meaning of thermoelectric power for single-crystal and polycrystalline specimen of the same compound is different. In the latter case, the thermoelectric power data are strongly influenced by the microstructure.

The thermopower data indicate that TiO_2 at high $p(O_2)$ is a p-type semiconductor. The $p(O_2)$ related to the n−p transition increases with increase of temperature. The formation of the p-type TiO_2 for the high-purity specimen studied in the present work is evidence for the presence of titanium vacancies. In the case of typical experimental conditions, the concentration of these titanium vacancies remains constant and is practically independent of $p(O_2)$ in the gas phase. Their transport kinetics will be considered in the Part IV of the present series.[22]

Acknowledgment. The present work was supported by the Australian Research Council, Rio Tinto Ltd., Brickworks Ltd., Mailmasters Pty. Ltd., and Sialon Ceramics Pty. Ltd.

References and Notes

(1) Nowotny, M. K.; Bak, T.; Nowotny, J. *J. Phys. Chem. B* **2006**, *110*, (Part I, jp0606210), 16270.

(2) Kofstad, P. *Electrical Conductivity, Diffusion and Nonstoichiometry of Binary Metal Oxides*; Wiley: New York, 1972.

(3) Matzke, H. J. In *Nonstoichiometric Oxides;* Sorensen, O. T., Ed.; Academic Press: New York, 1981; pp 189−210.

(4) Baumard, J. F.; Tani, E. *Phys. Status Solidi* **1977**, *39*, 373.

(5) Nowotny, J. In: *The CRC Handbook of Solid-State Electrochemistry*; Gellings, P. J., Bouwmeester, H. J. M., Eds.; CRC Press: Boca Raton, FL, 1997; pp 121−159.
(6) Bak, T.; Nowotny, J.; Sorrell, C. C.; Zhou, M. F. *J. Mater. Sci.: Mater. Electron.* **2004**, *15*, 645.
(7) Nowotny, J.; Radecka, M.; Rekas, M. *J. Phys. Chem. Solids* **1997**, *58*, 927.
(8) Kuratomi, T.; Yamaguchi, K.; Yamawaki, M.; Bak, T.; Nowotny, J.; Rekas, M.; Sorrell, C. C. *Solid State Ionics* **2002**, *154*−*155*, 223.
(9) Bak, T.; Burg, T.; Kang, S.-J. L.; Nowotny, J.; Rekas, M.; Shepard, L.; Sorrell, C. C.; Vance, E. R.; Yoshida, Y.; Yamawaki, M. *J. Phys. Chem. Solids* **2003**, *64*, 1089.
(10) Nowotny, M. K.; Bak, T.; Nowotny, J. *J. Phys. Chem. B* **2006**, *110*, (Part III, jp060623k), 16292.
(11) Jonker, G. H. *Philips Res. Rep.* **1968**, *23*, 131.
(12) Bak, T.; Nowotny, J.; Rekas, M.; Sorrell, C. C. *J. Phys. Chem. Solids* **2003**, *64*, 1057.
(13) Cusack, N.; Kendall, P. *Proc. Phys. Soc., London* **1958**, *72*, 898.
(14) Nowotny, M. K.; Bak, T.; Nowotny, J.; Sorrell, C. C. *Phys. Status Solidi* **2005**, *242*, R88.
(15) Burg, T., Ph.D. Thesis, School of Materials Science and Engineering, University of New South Wales, in progress.
(16) Parravano, G. G.; Domenically, C. A. *J. Chem. Phys.* **1957**, *26*, 359.
(17) Wynblatt, P.; McCune, R. C. In *Surface and Near-Surface Chemistry of Oxide Materials*; Elsevier: Amsterdam, 1988; pp 247−280.
(18) Stoneham, A. M. *Phys. Today* **1980**, January, 34−42.
(19) Nowotny, J. In *Science of Materials Interfaces*; Elsevier: Amsterdam, 1991; pp 79−209.
(20) Balachandran, U.; Eror, N. G. *J. Mater. Sci.* **1988**, *23*, 2676.
(21) Chan, N. H.; Sharma, R. K.; Smyth, D. M. *J. Amer. Ceram. Soc.* **1981**, *64*, 556.
(22) Nowotny, M. K.; Bak, T.; Nowotny, J. *J. Phys. Chem. B* **2006**, *110*, (Part IV, jp060624c), 16302.